Compact optical coherent receiver for avionics applications

S. Ayotte*, M. Morin, P. Deladurantaye, G. Bilodeau, L.-P. Perron,
F. Costin, A. Babin, G. Brochu, J. Blanchet-Létourneau, C.-A. Davidson,
D. D'Amato, É. Girard-Deschênes, P. Chrétien, M. Laplante, M. Drolet
Teraxion, 2716 rue Einstein, Québec, Québec, Canada G1P 4S8

ABSTRACT

An optical coherent receiver for the down conversion of radio frequency (RF) signals from 10-18 GHz to 2 GHz is presented. Light from a distributed feedback semiconductor laser is split between two lithium niobate Mach-Zehnder modulators driven either by a tunable local oscillator (LO) tone or a RF signal coming, for example, from a receiving antenna. The modulated light signals are combined with an optical coupler and filtered by two fiber Bragg gratings (FBG) that select one optical sideband from each signal. Detection of the filtered light by a balanced photo-detector produces an electrical signal at an intermediate frequency equal to the beat difference between the RF and LO frequencies.

Most current RF photonic systems are made from individually packaged devices that are interconnected with fiber-optic cables. In order to reduce size and weight and make the coherent receiver suitable for use in smaller airborne and mobile platforms, optical and opto-electronic components are packaged within a common enclosure where light routing is performed by micro-optics. A printed circuit board (PCB) is included within the module. It comprises a micro-processor to control and monitor the laser, the FBGs and thermo-electric coolers to ensure a robust operation over time and fluctuating environmental conditions. The module including the PCB, laser, modulators, optics, optical filters and balanced detector has a size of 89 x 64 x 32 mm^3.

Keywords: RF photonics, optical coherent receiver, tunable receiver, frequency downconversion, photonic downconversion, photonic mixer, micro-optics, avionics

1. INTRODUCTION

Radio-frequency (RF) photonics, whereby RF signals are propagated and processed in the optical domain, offer many advantages over conventional RF technology[1]. The frequency of an optical carrier (e.g. 193.5 THz at 1.55 μm), being orders of magnitude larger than that achievable in the RF domain, greatly facilitates addressing high frequency and large bandwidth signals. Other than this fundamental gain in performance, RF photonics brings about many practical advantages. All RF bands of interest can be addressed with a single optical platform. Optical fiber cables used to transport signals in RF photonics systems afford a sizable reduction in weight and orders of magnitude reduction in attenuation at GHz frequencies in comparison to RF cables. They are also immune to electromagnetic interference. As a result, RF photonics systems provide higher performance at a lower size, weight, and power (SWaP) than traditional electrical systems, features that are highly desirable especially for avionics applications.

Most current RF photonic systems are made from discrete and individually packaged devices that are interconnected with fiber-optic cables. The SWaP of these systems limits their use in smaller airborne and mobile platforms. A different approach has been followed to overcome these limitations, whereby all optical and optoelectronic components are encapsulated in a common package. The system under consideration is a tunable frequency downconverter[2]. It can receive high-frequency (up to tens of GHz) analog RF signals, from an antenna in the wing of an aircraft for example, and downconvert the information from one of many RF subcarriers to lower frequencies compatible with analog to digital converters. This receiver comprises a distributed feedback semiconductor laser (DFB), two lithium niobate Mach-Zehnder modulators (MZMs), two fiber Bragg gratings (FBGs) and a balanced photo-detector. Free space micro-optics directs light from one component to the next. Such hybrid technology, whereby components made from different materials are combined, is prevalent in commercial photonic products made in high-volume automated production lines.

* sayotte@teraxion.com; phone 1-418-658-9500; www.teraxion.com

2. PRINCIPLE OF OPERATION

The configuration of the receiver is illustrated in Figure 1. Light from a narrow linewidth laser is split equally between two Mach-Zehnder modulators (MZM) driven in a push-pull mode and operated at a null bias point. In the absence of any driving signal, light transmission by the modulators is the minimum afforded by their finite extinction ratio. This has the advantage of limiting the power of the laser optical carrier downstream from the modulators. One modulator is driven by a received RF signal, while the other one is driven by a pure local oscillator (LO) tone. The outputs from the modulators are then mixed by a 2x2 coupler and focused in two optical fibers leading to circulators and fiber Bragg grating (FBG) filters. Light reflected by the FBGs is finally detected by a balanced photo-detector. Balanced photo-detection rejects common mode noise resulting from the laser intensity noise (RIN) and doubles the optical power being detected, which translates into a 6 dB increase in the RF gain. The signal is finally amplified by an IF amplifier.

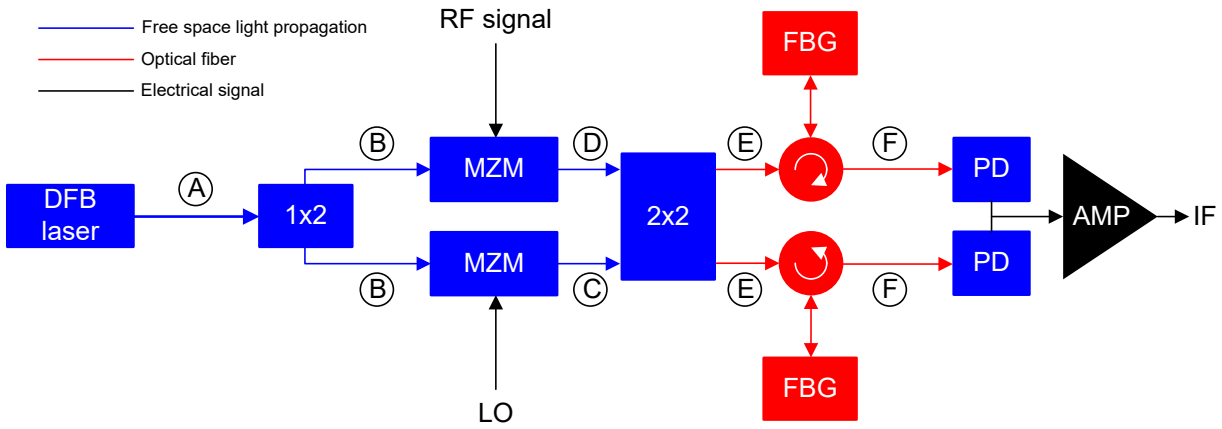

Figure 1. Configuration of the tunable coherent receiver.

The operation of the receiver can be understood by considering the evolution of the optical power spectrum from one component to the other as illustrated in Figure 2. Light emitted by the DFB laser and reaching both modulators is essentially monochromatic with an optical carrier frequency v_{laser} (power spectra A and B). Intensity modulation by a MZM diverts light from the laser carrier to optical sidebands. The LO modulator should be driven hard enough to maximize the amplitude of the first sidebands located at optical frequencies $v_{laser} \pm f_{LO}$, f_{LO} being the RF frequency of the local oscillator. Power spectrum C is representative of the optical power spectrum leaving the LO modulator under this condition. In the case of a modulator driven in a push-pull mode around a null bias point, even sidebands are limited by the extinction ratio of the modulator, which explains the weakness of the optical carrier and of the second sidebands located at $v_{laser} \pm 2f_{LO}$.

The RF input to the receiving modulator can comprise many signals transported over distinct subcarriers. Each signal can produce multiple sidebands on both sides of the optical carrier. In order to minimize inter-signal interference, their amplitude at the MZM modulator should be low enough that each signal diverts significant optical power towards first sidebands only. Under this condition, light leaving the signal modulator comprises sidebands at optical frequencies $v_{laser} \pm f_{RF\text{-}n}$ where $f_{RF\text{-}n}$ is the n^{th} RF subcarrier frequency as shown in spectrum D. The optical signals leaving the 2x2 coupler obviously carry a mixture of spectra C and D. Finally, each FBG is tuned to reflect only a first sideband of the LO and a neighboring sideband from one RF signal as shown in spectrum E. The interference of these sidebands produce upon photo-detection an electrical signal centered on an IF frequency equal to $|f_{LO} - f_{RF\text{-}n}|$. For example, a local oscillator at 16 GHz down converts a RF signal at 18 GHz to an IF frequency of 2 GHz thus easing its processing in the electrical domain.

Tuning of the receiver requires two actions. Firstly, the local oscillator must be tuned close enough to a RF subcarrier to be detected to ensure that their frequency difference is smaller than the FBG reflection bandwidth and smaller than the receiver photodetection bandwidth. Secondly, these sidebands must be aligned optically with the reflectivity spectrum of the FBGs. To this end, either the laser frequency of oscillation v_{laser} or the FBGs can be tuned thermally.

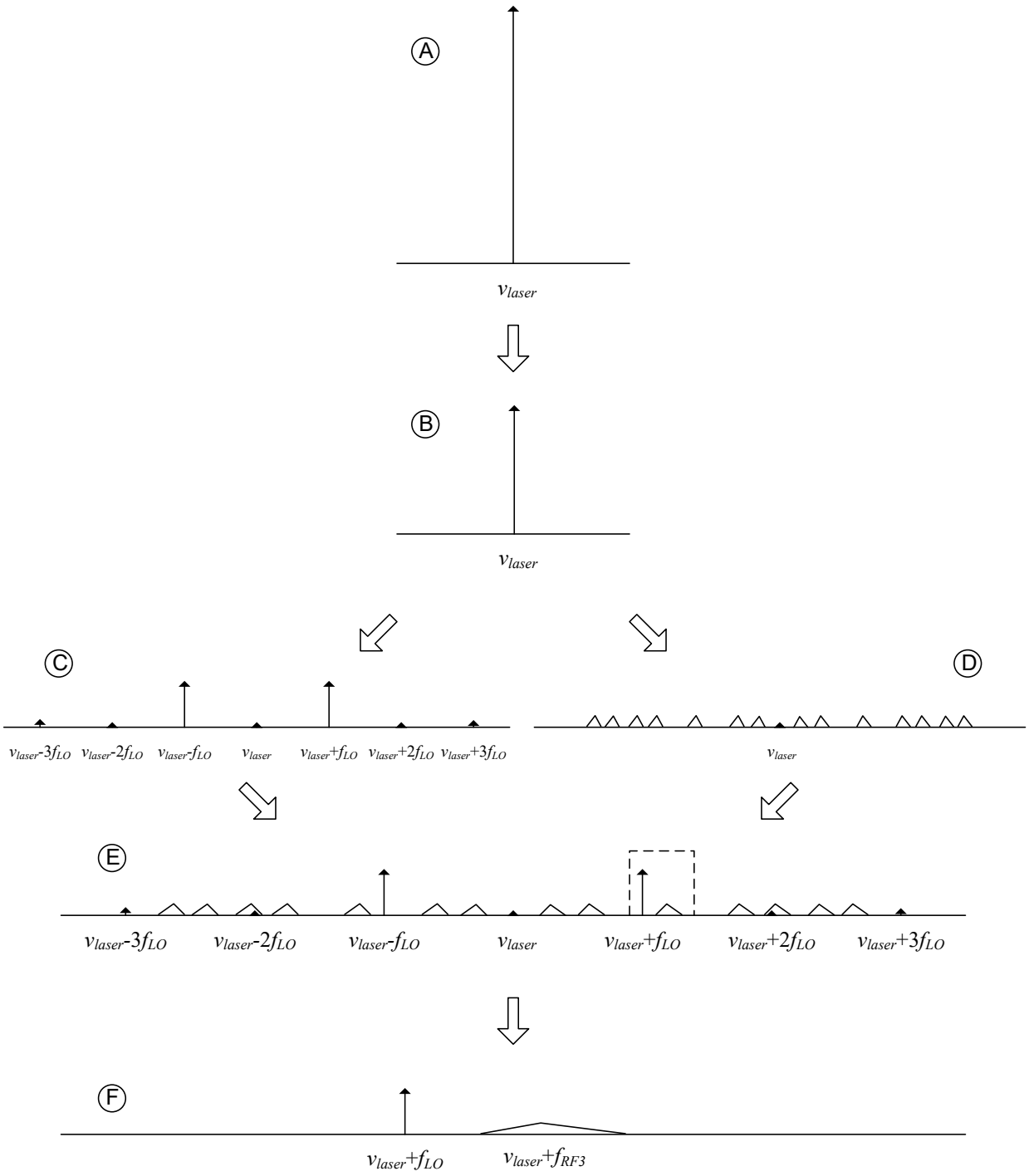

Figure 2. Evolution of the optical power spectrum within the receiver, when the receiver is tuned to receive the signal carried by the third subcarrier at frequency f_{RF3}.

3. RECEIVER CONSTRUCTION

The light source is a 1.55 µm DFB semiconductor laser that can provide over 100 mW of optical power with a linewidth smaller than 1 MHz. The lithium niobate Mach-Zehnder modulators (MZM) are capable of handling up to 100 mW of optical power. They have an electro-optic bandwidth of 20 GHz at 3 dB and an extinction ratio better than 20 dB. The fiber Bragg grating (FBG) filters have a maximum reflectivity of 94% and a bandwidth of 10 GHz. The balanced photo-detector has a responsivity of 1 A/W and an electrical bandwidth of 2.5 GHz.

As indicated in Figure 1, free-space optics is used except to couple light in and out of the FBGs. The output beam from the laser first goes through a sub-assembly comprising a micro-lens, a micro-isolator and a grin lens. The collimated light beam is redirected and split between two paths with prism towers and focused by micro-lenses in the Mach-Zehnder modulators. Light exiting each modulator is collimated by a micro-lens and partially reflected by a cube beam splitter. Each pick-up beam thus produced carries 5% of the incoming power and is focused by a 1 mm lens on a photodiode, the resulting detection signal being used to control the bias point of the modulator. The main beams exiting the cube beam splitters are recombined on two common paths with an optical flat and a TIR prism. The recombined beams are then focused by micro-lenses into the optical fibers leading to the optical circulators and FBGs. The design of this complex optical sub-assembly was carried out with commercial software to minimize insertion loss and equalize path lengths. Ray tracing diagrams of the input optics between the laser and the modulators and of the output optics between the modulators and the optical fibers are shown in Figure 3. The path lengths between the laser and the optical fibers are by design equalized to better than 20 ps.

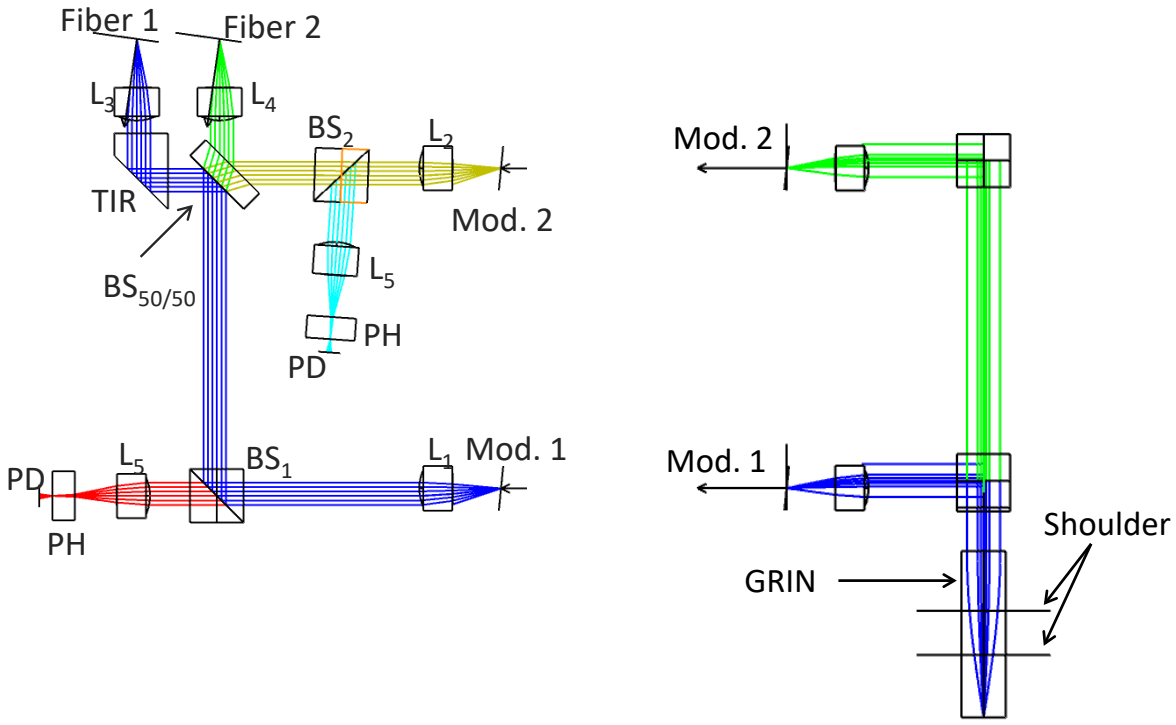

Figure 3. Ray tracing diagrams of the input optics between the laser and the modulators (right) and the output optics between the modulators and the optical fibers (left).

The receiver module further comprises RF transmission lines mounted on ceramics to carry the driving signals from GPPO input connectors to the modulators. The lines were designed to be as straight as possible, hence minimizing RF losses at GHz frequencies. Figure 4 presents the frequency response of the modulators calculated with commercial RF modeling software, taking into account the GPPO input connector to the receiver, the RF transmission line leading to the modulator, as well as the S-parameters of the modulator itself. The insertion loss is expected to remain below 9 dB at a frequency of 40 GHz. At 20 GHz, 3 dB of the insertion loss originate from the modulator.

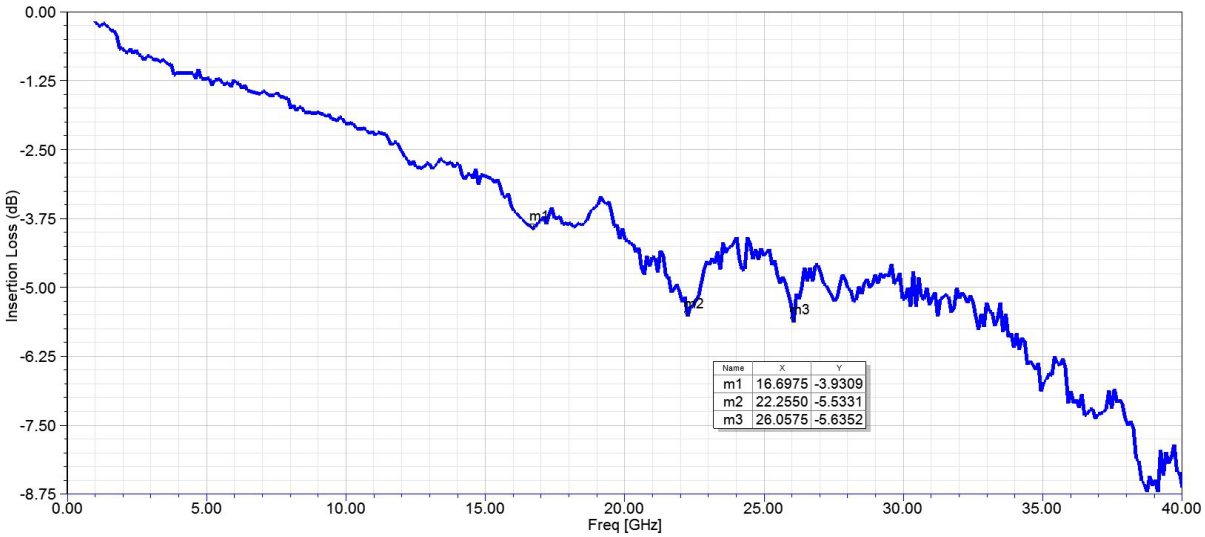

Figure 4. Frequency dependence of the RF insertion loss to the modulators.

The laser, each FBG and the pair of modulators are mounted on independently controlled thermo-electric coolers (TECs) to ensure a robust operation over time and fluctuating environmental conditions. The TECs are driven by a printed circuit board (PCB) comprising also a micro-processor for control and monitoring. The electrical interconnections between the laser, the modulators, the balanced photodiode and the PCB are made by gold wire bonds. Figure 5 presents photographs of the RF photonic receiver. The complete module including all of the above optical and electrical components, as well as the IF amplifier indicated in Figure 1, occupies a volume of 89 x 64 x 32 mm^3. This represents a significant reduction in volume compared to existing systems based on discretely packaged optical components. This gain in compactness is afforded by the use of unpackaged laser, modulators and balanced photo-detector allowing their encapsulation in a common enclosure. The receiver operates on 5 W of electrical power. The table below compares the SWaP of a typical receiver made from discrete components to that of the current hybrid receiver.

Table 1. Comparison of the SWaPs of the current hybrid receiver and of a typical receiver made from discrete components.

Parameter	Discrete	Hybrid	Unit
Volume	600	11	Cubic inches
Fiber	100	17.5	Feet
Fusion splices	20	6	
Connectors	20	0	
Weight	15	1.2	Pounds
Power	100	5	Watts

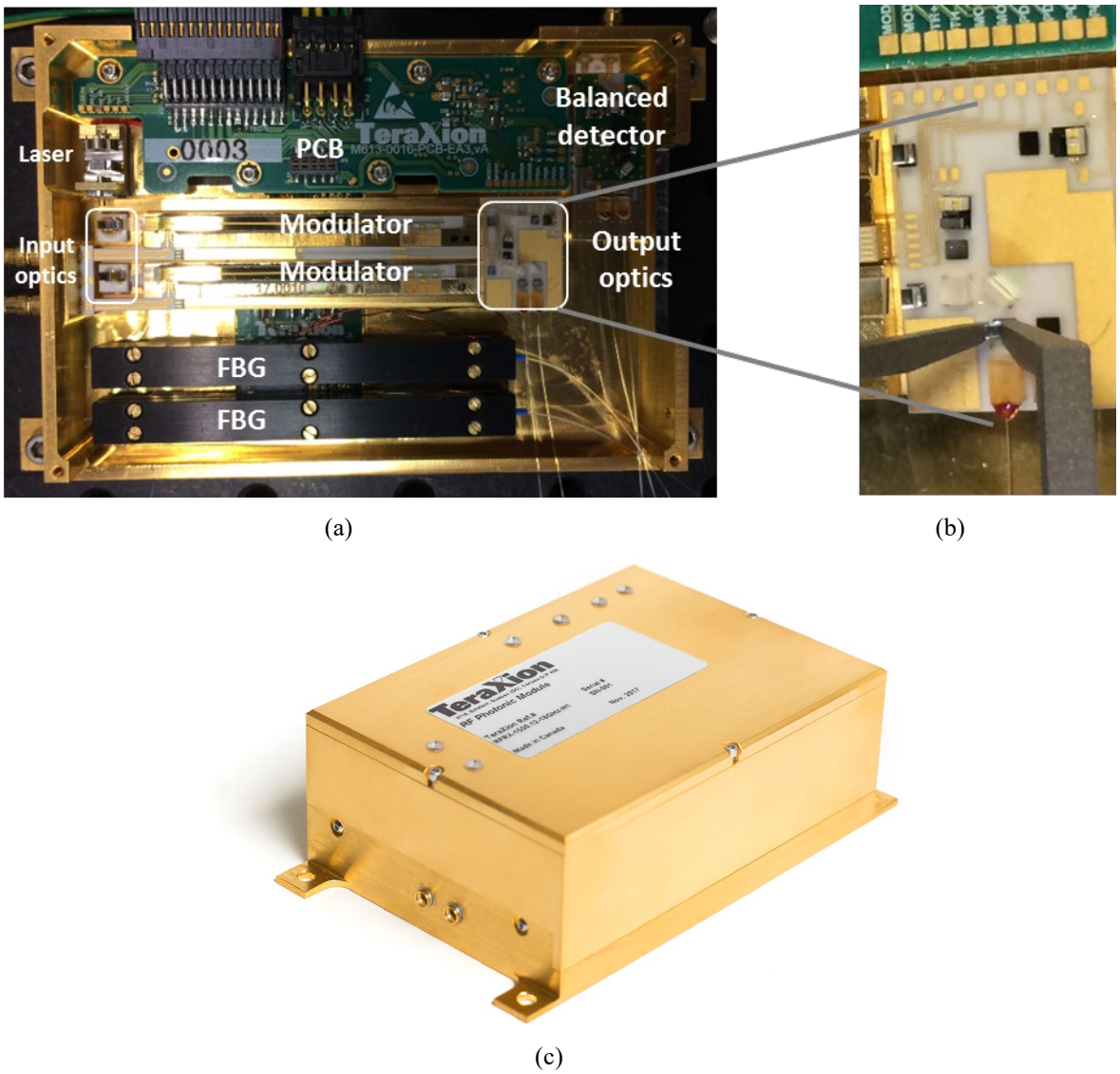

(a) (b)

(c)

Figure 5. Photographs of the tunable coherent receiver. (a) Components located inside a common enclosure. (b) Optical component of the output optics being positioned with a precise gripper. (c) Closed receiver module.

4. EXPERIMENTAL RESULTS

A prototype as described has been built and characterized. The measured optical insertion optical loss from the laser to each optical fiber, including the coupling loss into the fiber, amounts to 16 dB for light travelling through the LO modulator and 13 dB for light travelling through the RF signal modulator. An insertion loss of 13 dB was expected from simulations assuming an optimal alignment and a 3.5 dB loss for the modulator. The insertion loss along an optical fiber path including a circulator and a FBG was measured to be 4.1 dB. This measurement was performed with three fiber connectors in place on each fiber path. Replacing the connectors by splices reduced these losses by about 0.4 dB and allowed a fiber path equalization of 11.1 ps. This was assessed by comparing the phase of the signals produced by each photodiode upon receiving intensity-modulated light produced by one MZM operated at quadrature and driven by a single tone. During these measurements, each photodiode of the balanced photo-detector was illuminated individually by aligning spectrally with the incoming light only that FBG to which it is associated.

The loss affecting the RF signals driving the MZMs were evaluated by measuring the optical spectrum at the output of each modulator and calculating the ratio of the first and third modulation sideband powers, equal theoretically to

$$J_1^2(\beta)/J_3^2(\beta) \tag{1}$$

J_n being the Bessel function of the first kind and order n and modulation index β being equal to

$$\beta = \frac{\pi}{V_\pi}\sqrt{\frac{R_{MZM}P_{RF}}{2}} \tag{2}$$

where R_{MZM} is the RF input impedance of the modulator and P_{RF} is the effective RF power driving the modulator voltage. The RF loss is determined by comparing power P_{RF} deduced from the preceding expressions to the actual RF power input to the receiver. For example, at a RF input power of 22 dBm and a frequency of 16 GHz, the LO modulation index amounted to 0.72, well below the optimal value of 1.84 maximizing first order sidebands. Assuming a half-wave voltage V_π of 5.2 V and input impedance R_{MZM} of 50 Ω, this translates into a RF loss of 4.4 dB. The RF loss on the RF signal modulator at 18 GHz was similarly measured to be 5 dB. The RF and LO input powers were measured at the SMA connectors of short coaxial SMA-GPPO adaptor cables connected to the GPPO input connectors of the receiver. These cables and GPPO connections add about 0.7 dB loss to RF signals fed to the receiver that would be absent under normal use. Adding these to the loss predicted in Figure 4 at 16 and 18 GHz, 4.5 dB of RF loss are expected, in fairly good agreement with the measured values.

Figure 6 presents the IF output power at 2 GHz measured as a function of the RF input power at two different RF signal frequencies (10 or 18 GHz) and with two laser output powers (88 mW or 149 mW obtained at a drive current of 300 mA or 500 mA, respectively). The right graph presents the associated RF gain of the receiver, defined as the ratio between the IF output power and the RF input power. These gains include 15.5 dB of gain provided by the IF amplifier. The laser power increase from 88 to 149 mW translates into a 5.1 dB increase in RF gain, whereas a gain increase of 2 dB per dB of laser power is expected from theory (i.e. 4.6 dB in the present instance). Increasing the RF and LO frequencies from 10 and 8 GHz to 18 and 16 GHz, respectively, decreases the RF gain by 3.5 dB. This results from the RF loss increase in driving the MZM modulators: a model taking into account the loss variation indicated in Figure 4 and a 0.2 dB loss increase in the SMA-GPPO cables predicts a RG gain decrease of 3.1 dB, in fairly good agreement with the measurement. Saturation of the RF gain becomes visible at a RF input power of 15 dBm.

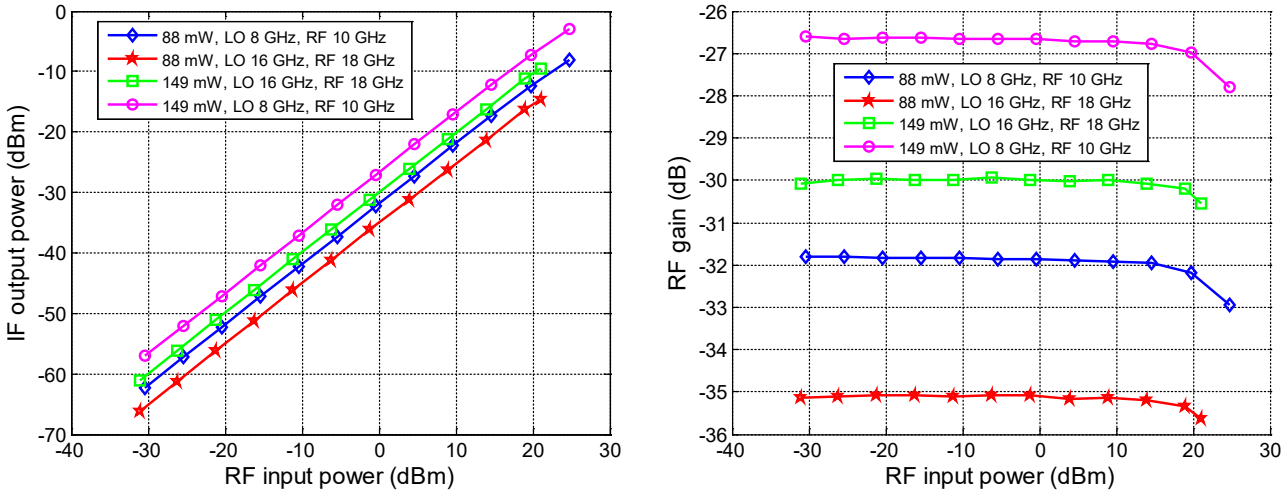

Figure 6. IF output power at 2 GHz measured as a function of the RF input power at either 10 or 18 GHz (LO: 22 dBm at 8 or 16 GHz, laser output power: 88 mW or 149 mW).

The RF gain of the receiver can be improved in a number of ways. As aforementioned, the measured modulation index of the local oscillator at a power of 22 dBm and 16 GHz amounted to 0.72 only. Operating at a modulation index of 1.84 instead would increase the RF gain by nearly 5 dB. Furthermore, optimizing the optical alignment in order to reduce the insertion loss on the LO modulator path to that achieved on the RF signal modulator path should provide a further gain increase of about 3 dB. Optimization of the splices on the optical fiber paths should likewise translate into a gain increase by a few dB. Headway could be made in the output stage as well. The balanced photodiode in the present prototype is terminated in a 50 Ω resistor connected to the system ground to match the IF amplifier input impedance of 50 Ω. With the right choice of IF amplifier and a design that minimizes the electrical distance between the balanced photo-detector and the IF amplifier, the termination resistor could be eliminated. This would avoid diverting half of the output current to the ground and allow increasing the RF gain of the receiver by 6 dB.

Two factors limit the frequency response of the receiver. Firstly, the efficiency in driving the modulators with RF signals decreases at high frequencies (see Figure 4), a mechanism that limits the accessible RF and LO carrier frequencies as evidenced in Figure 6. Secondly, the balanced photo-detector has a finite bandwidth, which limits the IF frequency that can be generated efficiently as well as the bandwidth of RF signals that can be received. Figure 7 presents the RF gain measured as a function of the IF frequency with a constant LO frequency of 10 GHz, a laser output power of 88 mW, and RF powers driving the LO and RF signal modulators of 22 dBm and 0 dBm, respectively. In this case, the photo-detector limited bandwidth contributes to the sharp decrease in the RF gain as the IF frequency increases beyond 2.5 GHz.

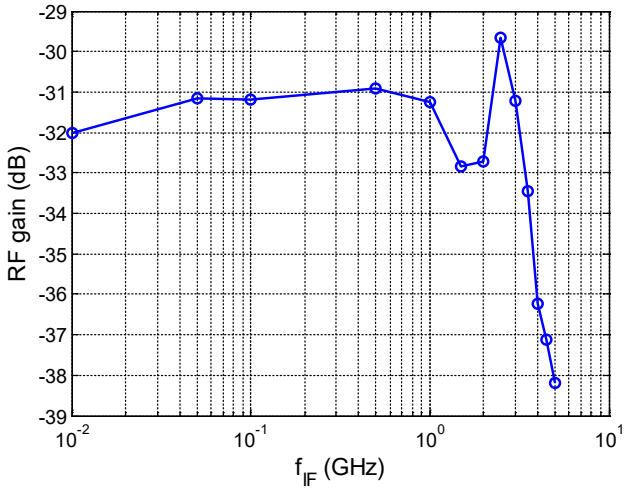

Figure 7. IF output power measured as a function of the IF frequency (LO: 22 dBm at 10 GHz, RF signal: 0 dBm at 10 GHz + f_{IF}, laser output power: 88 mW).

A perfectly linear receiver can be characterized by a linear frequency response, each frequency in the output signal being related solely to the same frequency in the input signal. In practice, nonlinearity in the receiver response produces some distortion of an incoming RF signal. In the frequency domain, this distortion manifests itself as intermodulation whereby frequencies from the input signal are mixed to produce outputs at different frequencies. In the present instance, the nonlinearity stems mostly from the MZM modulators. In order to quantify this effect, it is customary to examine the response of a receiver to a signal composed of discrete tones that are close to one another, these tones mimicking the frequency content of an incoming RF signal with a non-zero bandwidth. The nonlinearity of the present receiver has been characterized by driving the RF modulator with tones at 11.99 and 12.01 GHz, while the LO modulator was driven by a single tone at 11 GHz of 22 dBm. The linear response of the receiver generates beats at frequencies $f_{RF} - f_{LO}$, i.e. at 0.99 and 1.01 GHz. Tones at other frequencies are also observed in the output spectrum, the most significant ones being at $2f_{RF1} - f_{RF2} - f_{LO}$. In the present instance, these third order terms appear at 0.97 and 1.03 GHz, i.e. close enough to the desired beat frequencies to fall within the photodetection electrical bandwidth. Figure 8 compares the power of a linear tone (blue curve) to that of a third order term (red curve). As seen in this graph, the slope of the linear curve is unitary (in dB/dB), whereas that of the third order term is equal to three. The third order intercept (TOI) is defined as the point of

intersection of these linear extrapolations. In practice, a receiver is never operated at such high input powers at which nonlinear distortion would be devastating. The TOI is nonetheless used to quantify the nonlinearity of a receiver. The intercept point is located at an input power of 34.5 dBm and output power of 2.7 dBm. The noise floor (shot noise and thermal noise) after the IF amplification is visible at -154.7 dBm in a 1 Hz bandwidth. The total DC current produced by the balanced photodiodes then amounts to 0.3 mA.

Another metric of interest to characterize the performance of a receiver is the spur free dynamic range (SFDR), which depends on the noise level, the sensitivity and the nonlinearity of the receiver. As the power of the input signal is increased, the power of the linear output first rises above the noise floor. Increasing further the input power eventually leads to the third order term rising itself above the noise floor. The SFDR is defined as the range in input power over which these two events occur. It can be shown to be equal to

$$SFDR = \frac{2}{3}\left(OIP3(dB) - N_{total}(dB/Hz)\right) - 10\log_{10}(\Delta f^{2/3}) \qquad (3)$$

where *OIP3* is the output power at the third order intercept, N_{total} is the noise power spectral density and Δf is the detection bandwidth. According to Figure 8, the *SFDR* is equal to 105 dB in a 1 Hz bandwidth.

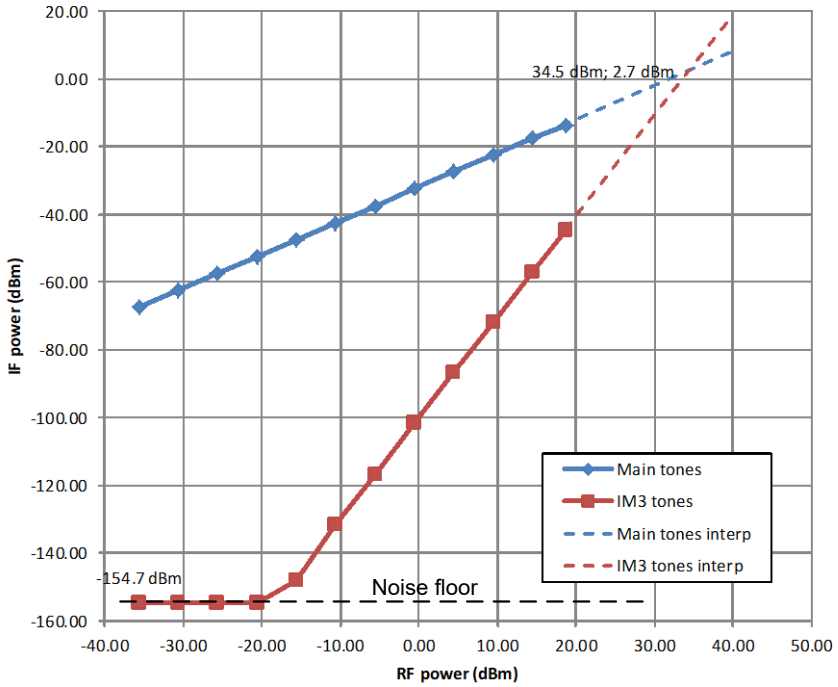

Figure 8. Output power of a linear tone (blue) and of a third order intermodulation product (red) as a function of the RF input power (LO: 22 dBm at 11 GHz, laser output power: 88 mW).

CONCLUSION

A compact optical coherent receiver has been designed, assembled and tested, that fits in 89 x 64 x 32 mm^3 form factor and operates with 5 watts of electrical power. Down conversion of signals in the 10-18 GHz band to an IF frequency of 2 GHz has been demonstrated. A RF gain of -30 dB has been achieved at an RF frequency of 18 GHz (LO @ 16 GHz). The measured SFDR in a 1 Hz detection bandwidth reaches 105 dB at an IF frequency of 1 GHz. This first receiver prototype has already demonstrated high performance at a SWaP highly advantageous for avionics applications. Desirable improvements have been identified and will be implemented in following units. They should lead to more than 15 dB increase in the RF gain.

ACKNOWLEDGEMENTS

TeraXion wishes to thank Harris Corporation and Ciena Canada for their technical contribution to this work. TeraXion acknowledges the financial support of Harris Corporation, and of the Government of Quebec through the *Greener Aircraft Catalyst Program SA²GE*.

REFERENCES

[1] Ridgway, R. W., Dohrman, C. L. and Conway, J. A., "Microwave Photonics Programs at DARPA," J. Lightwave Technol. 32(20), 3428-3439 (2014).

[2] Paolella, A. C., "Hybrid integration of RF photonic systems," IEEE Avionics and Vehicle Fiber-Optics and Photonics Conference (AVFOP) 2017, 29-30 (2017).